Very broad-band modeling of the 2004 Sumatra Earthquake: Towards modeling finite faults using the adjoint wave field

Vala Hjörleifsdóttir, Jeroen Tromp, Chen Ji, Qinya Liu, Hiroo Kanamori, Alex Song

Seismological Laboratory, California Institute of Technology, Pasadena, California 91125

Email: vala@gps.caltech.edu

1 Very broad-band modeling of the 2004 Sumatra Earthquake

1.1 Introduction

The December 26th, 2005, giant Sumatra-Andaman earthquake is the largest since the sixties and the first to occur after the advent of broad-band instruments and modern computational tools. A detailed investigation of the rupture process of this rare event is important to the understanding of the physics earthquakes.

The earthquake had a long duration which caused an initial under estimate of the size. Here we present a slip model that successfully predicts seismic wave field in the period range 20-2500 seconds without invoking "slow slip". However, amplitudes of static displacements recorded at GPS sites are larger than those predicted by the model.

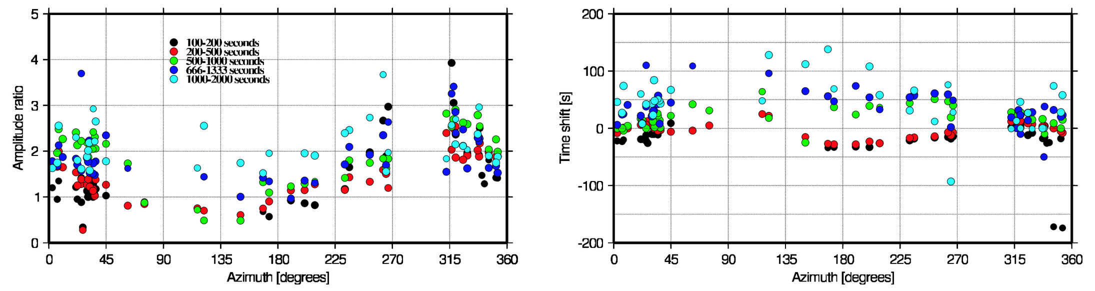

FIGURE 1: Amplitude ratios and time shifts between data and synthetics computed for the Harvard CMT. Note the change in oberved amplitude ratios and phase shifts with frequency.

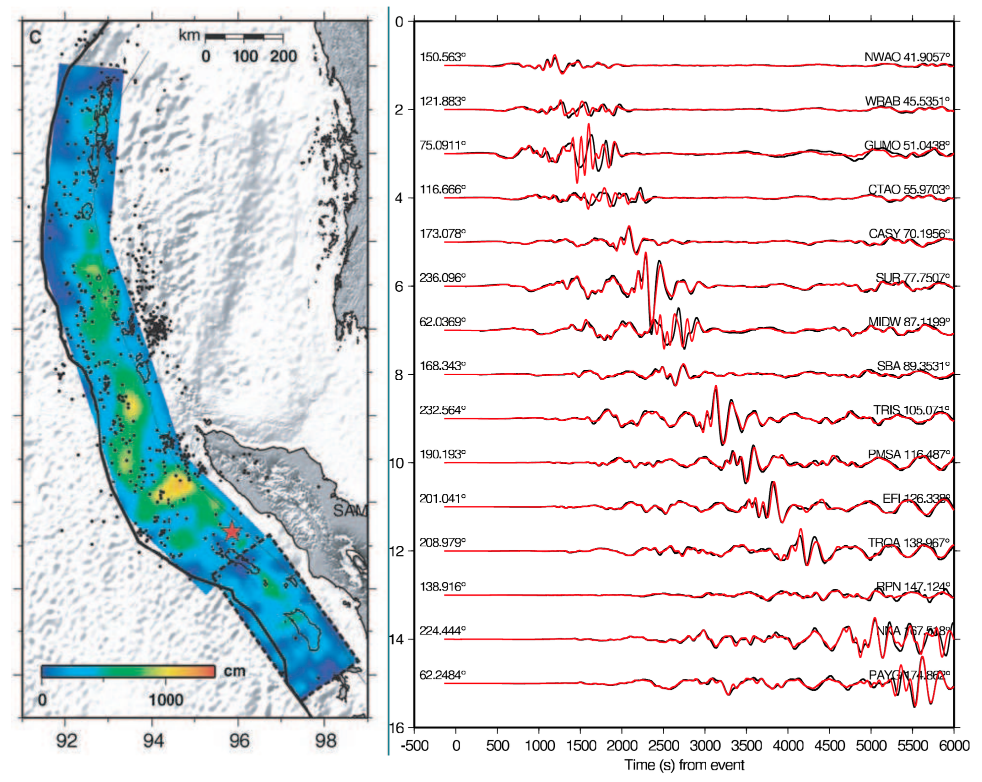

FIGURE 2: Slip distribution. The waveforms predicted by this model match observations well (Fig. 2). In particular the duration of the surface waves in Australia, which are especially sensitive to the directivity, is well matched.

1.2 Final solution

- Normal-mode Green's functions (periods of 20 seconds and longer).
- 600 second duration source.
- Teleseismic body waves
- 4 regional and 22 very broad-band (250-2000 sec) waveforms and 1 GPS vector (SAMP).
- Timing of regional waveforms calibrated by 3D SEM waveforms.
- Model iteratively improved by forward predicting long-period waveforms and normal-mode amplitudes.

The final model (Fig. 3) has a moment of $6.5 * 10^{29}$ dyne-cm and a rupture velocity of 2.5 km/s. Amplitude ratios and phase shifts are now reasonably constant over a wide frequency range and normal modes are explained to within 10% (*Park et al.*, 2005).

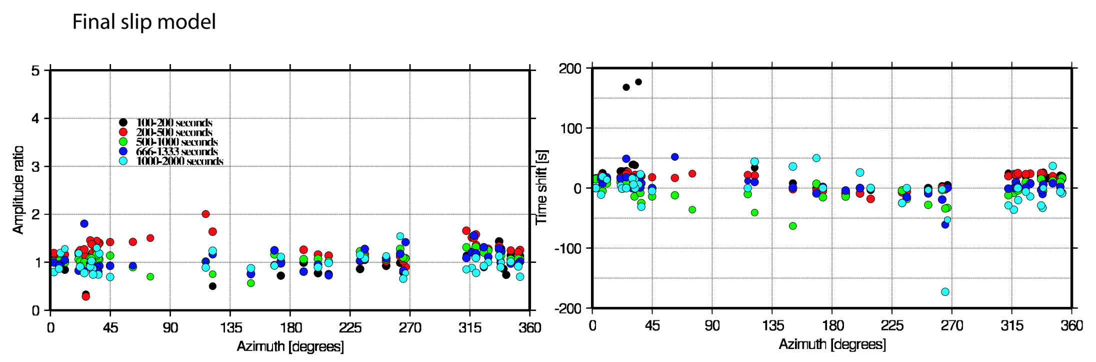

FIGURE 3: Amplitude ratios and time shifts between data and synthetics computed for the final source model are close to 1 and 0 respectively, for a wide range of frequencies.

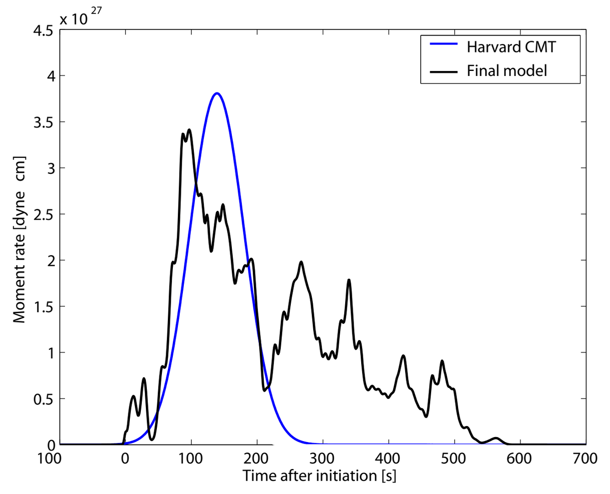

FIGURE 4: Moment rate function for Harvard CMT, preliminary source model and final source model. The CMT source matches the first part of the moment-rate function.

1.3 The Static Field

The slip model presented in the previous section can explain the seismic data over the observed frequency range. However, work on far-field static offsets (*Banerjee et al.*, 2005) proposes significantly larger slip than our model. Here we estimate the static offsets from our 3D SEM synthetics by averaging the displacement in a 2000 second long time window after the passing of the surface waves (Fig. 6 and Fig. 7). The far-field GPS data is matched within error bars, by this slip model, but the near-field data is severely underpredicted.

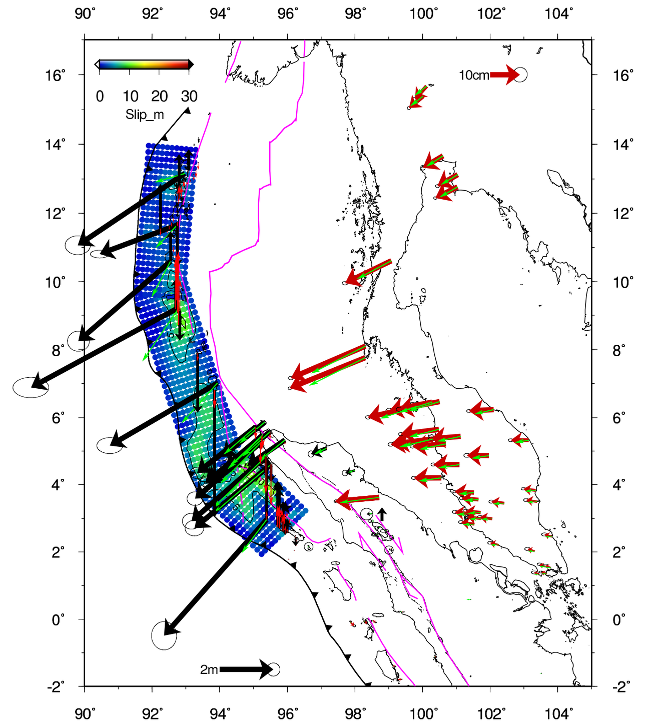

FIGURE 5: From Mohamed Chlieh: Static offsets from GPS campaign data in the Andaman and Nicobar Islands and continuous data from Thailand compared to predictions of the slip model. The vectors in the Andaman segment are underpredicted by almost a factor of 3, whereas the "intermediate" field is fairly well matched.

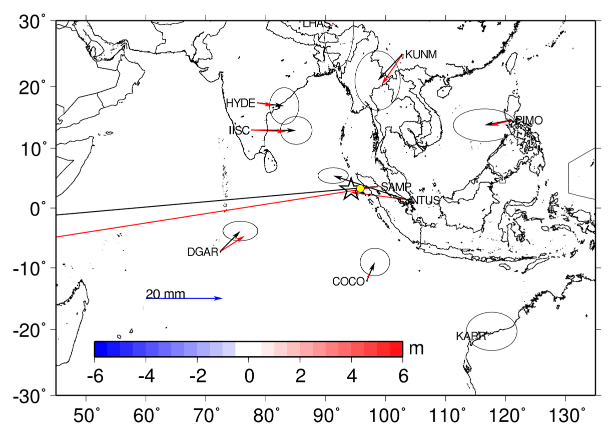

FIGURE 6: Static offsets at GPS stations as reported by *Vigny et al.* (2005) (black arrows) and computed by a 3D SEM simulation (red) for the final source model. The farfield GPS vectors are matched to within the error bars.

1.4 Conclusions

The Sumatra-Andaman earthquake broke more than 1200 km of the subduction zone and had a moment of $6.5 * 10^{29}$ dyne-cm. Most of the slip occured over 600 seconds. The presented slip model matches all the data available, except for the near-field GPS data. This is most probably caused by difference in timescale of the measurements as well as trade-offs between depth and structure for the far-field data.

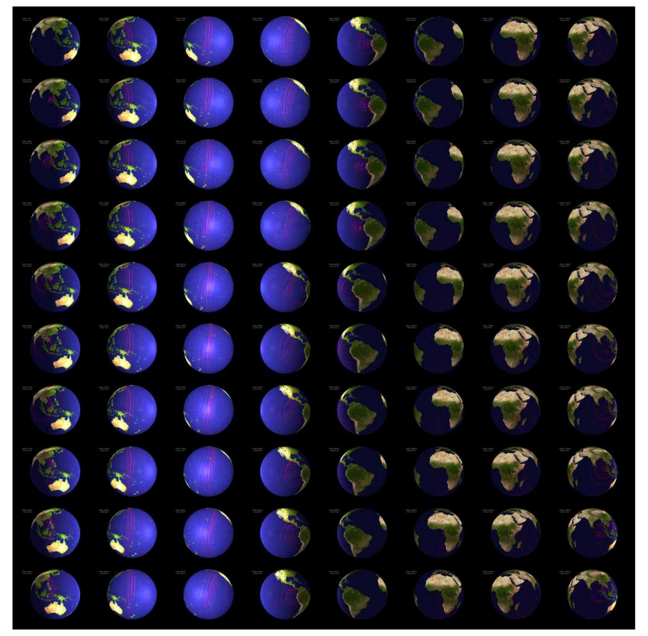

FIGURE 7: Snapshots from an SEM simulation. Movies of the wavefield, velocity and displacement can be found on our website: http://www.gps.caltech.edu/~vala/sumatra/ . These were made with help from Santiago Lombeyda at CACR.

2 Adjoint modeling of finite faults

For the giant Sumatra Earthquake it proved critical to use waves in a wide frequency band to constrain the source process. Currently, most investigators use isolated parts of the waveforms to invert for source structure to minimize the effect of 3D velocity structure. We are developing a method that utilizes 3D synthetic waveforms to invert for the source process, enabling us to use a greater part of the waveforms.

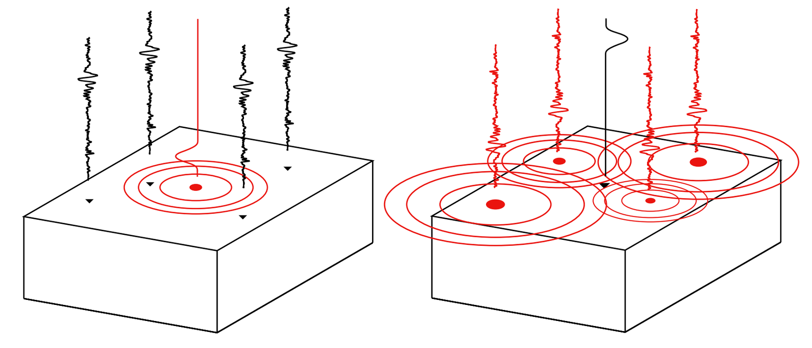

FIGURE 8: The adjoint wavefield can be created by inserting the seismograms recorded at each station, reverse in time, as simultaneous sources. The waves emanating from the receivers then constructively interfere at the source.

Tromp et al. (2005) illustrate how a (finite) source inversion may be implemented based upon the adjoint wave field. This wave field can be computed using the time-reversed difference between data and synthetics, estimated at all receivers, as simultaneous sources, and recording the resulting motions in a region around the fault plane. One can also back-propagate the data directly, in which case the waves emanating from all the "receivers" should collapse back on the origin point. The level of convergence will be determined by factors such as the source-receiver geometry, the frequency of the recorded data and synthetics.

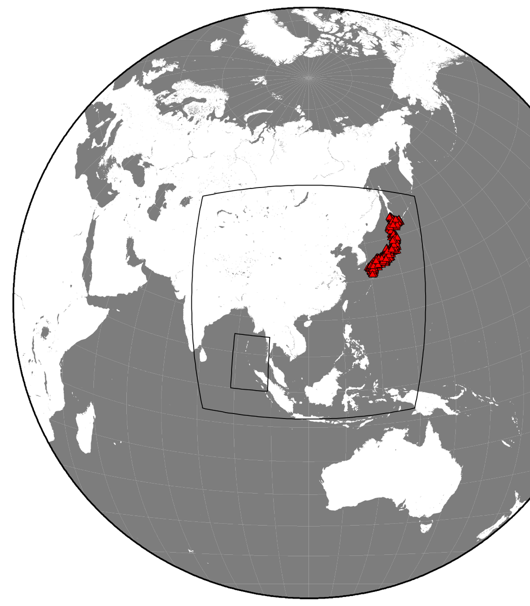

FIGURE 9: The relative location of the Sumatra source region and the Hinet Array. The larger black box shows the region of our proposed adjoint simulations.

The stacking method of *Ishii et al.* (2005) is a special case of this method where the Green's function from source to receiver is assumed to be a delta function with an p-wave arrival time given by a 1D reference model. By stacking the high frequency p-waves radiated from the Sumatra Earthquake at the HiNet array in Japan they can map the progression of the source. Fig. 2 shows our reproduction of their results.

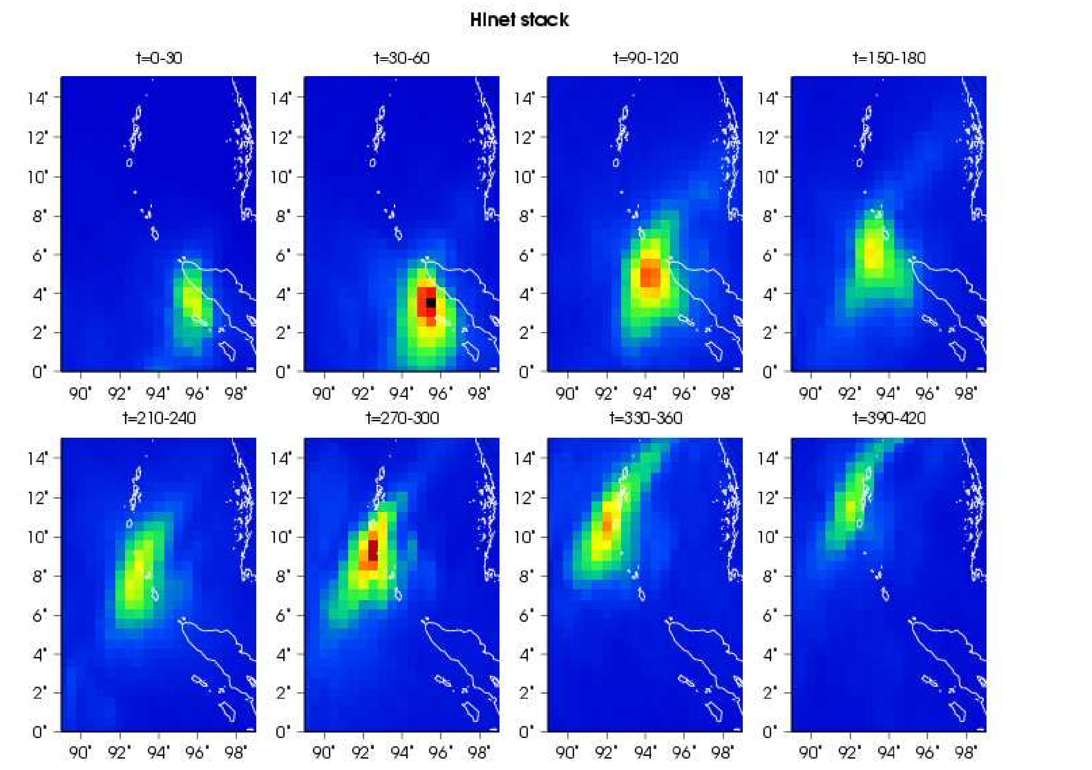

FIGURE 10: Maps showing the squared velocity of the stack produced for each source location, integrated over short windows The colors estimate how well the seismograms match up when assuming the source was in that particular pixel in that time window. The propagation of the "hot" patch shows the propagation of rupture.

We are currently working on back propagating the HiNet data as an example of the adjoint method, as it can easily be compared to the stacking results. The back-propagation method can be viewed as a sum over stacks over all rays within the seismogram, with the 3D Green's functions.

3 Acknowledgments

All the seismic data was downloaded from IRIS. This work was published in part in *Ammon et al.* (2005).

References

Ammon, C., et al., Rupture process of the 2004 Sumatra-Andaman earthquake, *Science*, *3*(5725), 1133–1139, 2005.

Banerjee, P., F. Pollitz, and R. Bürgmann, The size and duration of the Sumatra-Andaman arthquake from far-field static offsets, *Science*, doi:10.1126/science.1113746, 2005.

Ishii, M., P. Shearer, H. Houston, and J. Vidale, Extent, duration and speed of the 2004 Sumatra-Andaman earthquake imaged by the Hi-Net array, *Nature*, doi:10.1038/nature03675, 2005.

Park, J., et al., Earth's free oscillations excited by the 26 December 2004 Sumatra-Andaman earthquake, *Science*, *3*(5725), 1139–1144, 2005.

Tromp, J., C. Tape, and Q. Liu, Waveform tomography, adjoint methods, time reersal, and banana-doughnut kernels, *Geophys. Jour. Int.*, *160*(1), 195–216, 2005.

Vigny, C., et al., nsight into the 2004 Sumatra-Andaman earthquake from GPS measurements in southeast Asia, *Nature*, *436*, 201–206, 2005.